



PCCP

**Cooperatively enhanced hydrogen bonds in ionic liquids:  
Closing the loop with molecular mimics of hydroxy-  
functionalized cations**

Journal:	<i>Physical Chemistry Chemical Physics</i>
Manuscript ID	CP-ART-06-2019-003300.R2
Article Type:	Paper
Date Submitted by the Author:	29-Jul-2019
Complete List of Authors:	Niemann, Thomas; Universitat Rostock, Institute fur Chemie Strate, Anne; Universitat Rostock, Institute fur Chemie Ludwig, Ralf; Universitat Rostock, Institute fur Chemie Zeng, Helen; Yale University, Department of Chemistry Menges, Fabian; Yale University, Department of Chemistry Johnson, Mark; Yale University, Department of Chemistry

SCHOLARONE™  
Manuscripts

## Cooperatively enhanced hydrogen bonds in ionic liquids: Closing the loop with molecular mimics of hydroxy-functionalized cations

Thomas Niemann<sup>a,b</sup>, Anne Strate<sup>a,b</sup>, and Ralf Ludwig<sup>a,b,c,\*</sup>

<sup>a</sup>Department of Chemistry, University of Rostock, 18059 Rostock, Germany

<sup>b</sup>Department Life, Light & Matter – University of Rostock, 18051 Rostock, Germany

<sup>c</sup>Leibniz-Institut für Katalyse e.V., Albert-Einstein-Str. 29a, 18059 Rostock, Germany

Helen J. Zeng<sup>d</sup>, Fabian S. Menges<sup>d</sup>, and Mark A. Johnson<sup>d,\*</sup>

<sup>d</sup>Sterling Chemistry Laboratory, Yale University, New Haven, CT 06520, USA

**Abstract:** We address the cooperative hydrogen bonding interactions in play between the ionic constituents of ionic liquids (ILs) with particular attention to those involving the attractive interactions between two cations in the system 1-(2-hydroxyethyl)pyridinium tetrafluoroborate [HEPy][BF<sub>4</sub>]. This is accomplished by comparing the temperature-dependent linear infrared spectra of [HEPy][BF<sub>4</sub>] with that of the molecular mimic of its cation, 2-phenylethanol (PhenEthOH). We then explored the structural motifs of these H-bonded configurations at the molecular level by analyzing the cryogenic ion vibrational predissociation spectroscopy of cold (~35 K) gas phase cluster ions with quantum chemical methods. The analysis of the OH stretching bands reveals the formation of the various binding motifs ranging from the common <sup>+</sup>OH...BF<sub>4</sub><sup>-</sup> interaction in ion-pairs (c-a) to the unusual <sup>+</sup>OH...<sup>+</sup>OH interaction (c-c) in linear and cyclic, homodromic H-bonding domains. Replacing ion-pairs by the molecular (neutral) analogue of the IL cation also results in the formation of positively charged cyclic motifs, with the bands of the gas phase cationic cyclic tetramer (HEPy<sup>+</sup>)(PhenEthOH)<sub>3</sub> appearing quite close to those assigned previously to cyclic tetramers in the liquid. These conclusions are supported by density functional theory (DFT) calculations of the cationic and neutral clusters as well as the local structures in the liquid. Our combined experimental and theoretical approach for the gas and the liquid phases provides important insight into the competition between differently H-bonded and charged constituents in liquids.

The authors declare no conflict of interest.

\*To whom correspondence should be addressed. E-mail: ralf.ludwig@uni-rostock.de or mark.johnson@yale.edu

## Introduction

Hydrogen bonding is key to many processes in the chemistry and physical properties of molecular liquids,[1-10] and this interaction also plays an especially critical role in the rational design of ionic liquids (ILs), which solely consist of ions.[11-23] Coulomb enhanced hydrogen bonding between cation and anion in ILs has been examined in a plethora of infrared (IR) and Raman studies.[24-32] However, in the special case of hydroxy-functionalized ILs, two distinct types of H-bonds have been reported: one corresponding to the common, Coulomb-enhanced interaction between cations and anions (c-a), and a second that creates an attractive interaction between two cations (c-c).[33-41] For these ILs, structural motifs involving H-bonded cationic clusters were evidenced in the bulk liquid phase by means of linear infrared (IR) measurements, which displayed two distinct vibrational band envelopes that could be assigned to (c-a) and (c-c) hydrogen bond motifs. An interesting, and counterintuitive aspect of the (c-c) hydrogen bonds is that their characteristic OH stretching bands are more redshifted than those found in the (c-a) contacts, suggesting that the (c-c) bonds are stronger than those in the (c-a) case.[24-29] The formation of these (c-c) clusters is mediated by surrounding counter ions and was observed to become more prominent at lower temperature (~213 K).

Although it is expected that the H-bonds in ILs differ from those that are well studied in neutral clusters of water or alcohol molecules,[42-46] the diffuse nature of the vibrational bands from bulk ILs allows only a qualitative picture of the local interactions. Consequently, our recent classification of the broad, redshifted spectral bands of hydroxy-functionalized ILs to the formation of (c-c) dimers, trimers and cyclic tetramers was somewhat speculative, being guided primarily by DFT-calculated frequencies of related clusters.[34-37] Hence, the purpose of the present study is to combine linear infrared (IR) spectroscopy and cryogenic ion vibrational predissociation (CIVP) spectroscopy to quantify the spectral signatures of local (c-a), (c-c) and (c-m) [m = neutral molecule] H-bond motifs in ILs and molecular liquids (MLs) by comparing the bands in the liquid phase with those displayed by well defined, composition selected gas phase cluster ions. The combined experimental approach, together with quantum chemical calculations, provides a detailed understanding of the interplay among H-bonding interactions between cations, anions and neutral molecules and allows inferences to be made about the likely structural candidates that exist in the bulk.

## Strategy of this study

We illustrate the concept of this study in **Scheme 1**:

- (a) Temperature-dependent, low energy vibrational bands in the OH stretching region displayed by hydroxy-functionalized ILs are attributed to H-bond formation between cations, creating cationic clusters up to cyclic tetramers  $(c^+)_4(a^-)_4$  that are fully compensated by counter anions in the neutral bulk system.
- (b) Promote the formation of extended H-bond networks by replacing the ion-pairs  $(c^+)(a^-)$  by molecules (m) in IL/ML mixtures.
- (c) Isolate the spectral signatures of local H-bonding motifs in cold, gas phase ions with precisely controlled compositions with special attention to determine the intrinsic signatures of cyclic structures in the  $(c^+)(m)_3$  complexes.
- (d) Extend the gas phase cluster study to the  $(c^+)_4(a^-)_3$  cationic complex to compare with the bulk spectra from (a).

Our earlier studies showed that the formation of cationic clusters from ILs is enhanced by weakly interacting anions, polarizable cations with only one interaction site (e.g. one functional group) and large distances between the functional group and the positive charge centre of the cation.[34-39] For this reason, we have chosen the 1-(2-hydroxyethyl)pyridinium tetrafluoroborate [HEPy][BF<sub>4</sub>] (see **Scheme 2**) as a model IL to study. Specifically, the [HEPy][BF<sub>4</sub>] system provides a weakly interacting anion (BF<sub>4</sub><sup>-</sup>), a polarizable pyridinium ring (Py<sup>+</sup>), and a hydroxyethyl tether (HE) between the positively charged pyridinium ring and the OH functional group. This is in contrast to the situation in the 1-(2-hydroxyethyl)-3-methylimidazolium tetrafluoroborate [HEMIm][BF<sub>4</sub>] reported earlier, in which the acidic C<sub>(2)</sub>H at the imidazolium ring allowed for an additional interaction with the anion as well as with their own OH group or those of other cations, all interactions that would act to suppress cationic cluster formation.[38,39] The HEPy<sup>+</sup> cation in [HEPy][BF<sub>4</sub>], on the other hand, provides a single proton donor function with its OH group. To bridge the behavior of ionic liquids to their molecular analogues, we also follow the spectroscopic consequences when the IL cation is replaced by the 2-phenylethanol (PhenEthOH) molecular mimic. That modification was chosen because it likely acts to reduce the attractive and repulsive Coulomb forces at play in the systems and enhance the cooperative H-bond interactions for spectroscopic analysis. Such cooperative effects stem from non-pairwise-additive charge transfer and are characterized by strongly enhanced redshifts in IR spectra as observed with increasing size of water and alcohol clusters.[42-44]

## Features of cyclic cationic tetramers in the IR spectra of the ionic liquid [HEPy][BF<sub>4</sub>]

**Fig. 1** presents the infrared (IR) spectra of the pure IL [HEPy][BF<sub>4</sub>] as a function of temperature between 213 K and 353 K. To avoid congestion from aliphatic and ring CH vibrational bands and prevent possible overlap with strongly redshifted OH vibrational bands, these spectra are obtained after subtraction of that from the related OD functionalized IL. The OH group of the HEPy<sup>+</sup> cation provides hydrogen bonding either to the BF<sub>4</sub><sup>-</sup> anion, resulting in (c-a) clusters, and/or to the hydroxyl groups of other cations, giving (c-c) clusters. At the highest temperature (353 K), we observe a main OH vibrational band at 3549 cm<sup>-1</sup>, which can be easily assigned to the expected <sup>+</sup>OH...BF<sub>4</sub><sup>-</sup> hydrogen bond between the counter ions. The high wavenumber indicates that the cation-anion hydrogen bond is relatively weak in spite of the expected enhancement by their Coulombic attraction. In fact, the implied interaction strength is on the same order as those of water and methanol in similar ionic liquids with BF<sub>4</sub><sup>-</sup> anions.[18,19] However, the envelope of the observed vibrational band is not symmetric with extended intensity at the low frequency site. With decreasing temperature, this shoulder evolves into a distinct vibrational band with a maximum at about 3374 cm<sup>-1</sup> at 213 K while the main band redshifts by about 14 cm<sup>-1</sup>. In the usual scenario where H-bonds are expected to become stronger with decreasing temperature, the OH associated bands intensify and redshift. However, the growth of a distinct band redshifted by ~175 cm<sup>-1</sup> clearly indicates the formation of another class of bound OH groups, with candidates in this case likely corresponding to the (c-a) to (c-c) interactions. We note that overtone or combination bands can be excluded in this frequency range.[34]

Overall, the measured infrared spectra as a function of temperature are consistent with the formation of (c-c) hydrogen bonds, resulting in H-bonded clusters of like-charged ions. For the assignment of the measured IR spectra, we calculated two types of H-bonded clusters, (c-a) and (c-c), including up to four ion-pairs at the B3LYP-D3/6-31+G\* level of theory.[35-39] These structures were fully optimized and only positive frequencies were found indicating true minimum structures on the potential energy surface. For (c-a) clusters, only OH frequencies from H-bonding between cation and anion are present. Although we observe minor cooperative effects with increasing cluster size from the (c-a) monomer to the (c-a) tetramer, the calculated frequencies range between 3480 cm<sup>-1</sup> and 3620 cm<sup>-1</sup> and are contained within the width of the high energy band envelope with maximum at 3549 cm<sup>-1</sup>, which is therefore assigned to hydrogen bonding between cation and anion (see **Fig. 2**). As mentioned above, the OH frequencies are surprisingly high, considering that hydrogen bonding is enhanced by attractive

Coulomb interaction between cation and anion. The doubly ionic hydrogen bond is not stronger than the H-bond of an alcohol dimer.[42-45]

The linear clusters (c-c) are characterized by hydrogen bonding between the cations with the terminal OH group interacting with one of the anions leading to structural motifs  $^+\text{OH}\cdots^+\text{OH}\cdots\text{BF}_4^-$ . The DFT-calculated frequencies of the 2(c-c) dimer and the 4l(c-c) (linear (c-c)) tetramer reasonably describe the region of the broad redshifted vibrational band in the measured IR spectra with substantial intensity between  $3200\text{ cm}^{-1}$  and  $3480\text{ cm}^{-1}$ . However, the measured spectral band is best described by the calculated frequencies of a cyclic (4c(c-c)) tetramer, showing all the features of cyclic tetramers that have been reported earlier for water and methanol.[42-45] This agreement between the calculated frequencies of linear and cyclic (c-c) clusters with their neutral counterparts provides a compelling case that cyclic structural motifs are present in the ILs.

### **Enhanced cluster formation by adding the molecular liquid PhenEthOH**

Next, we test the hypothesis that addition of the molecular liquid PhenEthOH to the [HEPy][BF<sub>4</sub>] IL enhances the H-bonded domains. This was accomplished by monitoring the IR spectra resulting from various mixtures (0, 10, 20, 35 and 50 mol%) at  $T = 293\text{ K}$ , where only minor (c-c) cluster contributions are observed for the pure IL (see **Fig. 1**). The results are displayed in **Fig. 3**, demonstrating that the addition of PhenEthOH immediately results in substantial  $^+\text{OH}\cdots\text{OH}$  cluster formation, as evidenced by the rapid onset of the characteristic  $3374\text{ cm}^{-1}$  band observed earlier in the low temperature pure IL (**Fig. 1**). The calculated frequencies of the neutral tetramer clusters of the (c-c-m-m) and (c-m-c-m) configurations correspond well with this band region, with their structures displayed in **Fig. S1**. To provide more specific comparisons with the spectral signatures of these local motifs, we now turn to CIVP spectroscopy to establish the bands displayed by composition-selected cationic clusters of similar type.

### **Evidence for cyclic tetramers by means of cryogenic ion vibrational predissociation (CIVP) spectroscopy**

The spectral signatures of various H-bonded motifs can be directly accessed by measuring the vibrational spectra of cold, mass selected gas phase ions.[28] In the present case, we measured the spectra of the series  $(\text{HEPy}^+)(\text{PhenEthOH})_n$ , for comparison with the bands observed in the mixed IL/ML (**Fig. 3**).

The vibrational spectra of the mass selected ions were obtained using the so-called “messenger tagging” method.[52,53] In that approach, linear absorption spectra are acquired by monitoring photoevaporation of a weakly interacting adduct, in this case  $N_2$ , using a double focusing, tandem time-of-flight photofragmentation mass spectrometer described in detail previously.[54-57]

The spectral evolution of the cold ( $\sim 35$  K)  $(HEPy^+)(PhenEthOH)_n$  complexes ( $n = 1-3$ ) are compared with that of the isolated  $HEPy^+$  cation in **Fig. 4**. The doublet structure of the free OH peak is due to the perturbation by the  $N_2$  adduct as discussed in detail in **Fig. S2**. The important result is that the free OH peaks in the bare cation and binary complex (**Figs. 4a and 4b**) are clearly absent for the  $n = 2$  and 3 clusters (**Figs. 4c and 4d**), consistent with the formation of cyclic H-bond arrangements. Moreover, the band envelopes in the  $n = 2$  and 3 spectra fall just on the low energy side of the redshifted transitions observed in both the bulk IL at 213 K (**Fig. 4f**) and in the  $[HEPy][BF_4]/PhenEthOH$  mixture at 293 K (**Fig. 4e**).

The important advantage of comparisons with cluster results is that the isolated, cold systems can be accurately treated with electronic structure methods. This allows us to extract detailed structural information about how the local interactions are reflected in the spectra. The calculated (B3LYP-D3/6-31+G\*) structures and redshifts in the OH stretches of the  $(HEPy^+)(PhenEthOH)_{n=0-5}$  clusters are presented in **Figs. S3 and 5**, respectively.[40-43] These structures indeed correspond to homodromic H-bonded cyclic arrangements, which are analogous to those adopted by neutral cluster systems like methanol and water.[58,59] Such cycles are known to exhibit increasingly red-shifted OH stretching fundamentals with increasing size. The average (intensity-weighted) step-wise redshifts of the suite of OH vibrational transitions calculated for the cationic clusters are compared with the experimentally observed band energies in **Fig. 5**. This behavior provides strong evidence that the observed low energy features in the bulk spectra are indeed assigned to the formation of extended, cyclic H-bonded motifs.

The H-bonding propensities in the cationic networks are interesting in that they raise the issue of whether binary interaction between a cationic OH group acts preferentially as an H-bond donor or acceptor when interacting with a neutral alcohol. This issue is directly addressed in the  $(HEPy^+)(PhenEthOH)$  binary complex, where it can adopt two possible structures ( $^+OH\cdots OH$  vs.  $OH\cdots ^+OH$ ) which correspond to cationic H-bond donor and acceptor, respectively. The calculated bands of these combinations are compared to the neutral alcohol dimer,  $(PhenEthOH)_2$  (**Fig. 5**). The  $^+OH\cdots OH$  structural motif is characterized by significant charge transfer from the oxygen lone pair into the  $^+OH$  anti-bonding orbital, which is

particularly strong here because the OH belongs to the positively charged, and hence more acidic cation. In contrast, the  $\text{OH}\cdots^+\text{OH}$  linkage is weakened because the oxygen lone pair on the cation is less basic. Thus, the  $^+\text{OH}\cdots\text{OH}$  binary complex is the most energetically favorable configuration as opposed to  $\text{OH}\cdots^+\text{OH}$ , giving rise to a large redshift ( $260\text{ cm}^{-1}$ ) and is detected in the gas phase (**Fig. 4b**).

The character of the binary  $^+\text{OH}\cdots\text{OH}$  interaction has a profound impact on the spectrum of cyclic H-bonded networks that contain a single embedded cation, as the cation is a much better donor than it is an acceptor. This manifests as a splitting in the bands. Such an effect is illustrated by comparing the  $(\text{HEPy}^+)(\text{PhenEthOH})_3$  system with the symmetric (neutral)  $(\text{PhenEthOH})_4$  tetramer in **Fig. 6**. The single OH feature around  $3340\text{ cm}^{-1}$  that is calculated for the  $(\text{PhenEthOH})_4$  tetramer (**Fig. 6c**), splits into four distinct bands spanning a wide range between  $3231\text{--}3470\text{ cm}^{-1}$  (**Fig. 6b**). The lower energy bands correspond to displacement of the OH group on the cation, whereas the highest frequency transition belongs to the OH of the neutral molecule in the weak  $\text{OH}\cdots\text{OH}^+$  linkage (labeled  $\nu_{m_3}$  in **Fig. 6b**), discussed for the binary complex. Note that the dominant bands in the experimental spectrum for this cluster covers the same frequency range as the broad redshifted OH vibrational band of the 50 mol% IL/ML mixture (**Fig. 4e**), but appears  $\sim 90\text{ cm}^{-1}$  below that observed for the 213 K IL (**Fig. 4f**), which is also consistent with the elimination of the repulsive interactions in the gas phase species. Taken altogether, these observations provide compelling evidence for the formation of cyclic H-bonded domains in the bulk IL at low temperature (see **Scheme 1**), which would have been more challenging to accomplish by isolated, purely ionic complexes (**Fig. S4**).

## Conclusion

We analyzed liquid phase complexes and gaseous cationic clusters of  $[\text{HEPy}][\text{BF}_4]$  and the molecular mimic of its cation, 2-phenylethanol ( $\text{PhenEthOH}$ ) by means of infrared spectroscopy, cryogenic ion vibrational predissociation spectroscopy, and quantum chemical calculations. Theoretical analysis of the resulting infrared spectra reveals the assignments of the OH stretching bands to the different binding motifs. Dimers, linear and cyclic tetramers with (c-c) cooperativity were inferred based on the vibrational spectra of neat ILs, but the spectra of ternary cationic complexes in the gas phase were dominated by bands characteristic of the  $^+\text{OH}\cdots\text{BF}_4^-$  (c-a) interactions. However, replacing the ion-pairs with the molecular mimics of the IL cation yields features signalling OH network formation in both the positively charged cyclic tetramers  $(\text{HEPy}^+)(\text{PhenEthOH})_3$  and in mixtures of the ionic and molecular

liquids. Most importantly, the cationic cyclic tetramer  $(\text{HEPy}^+)(\text{PhenEthOH})_3$  exhibits vibrational bands in the OH stretching region that are similar to those previously-assigned[35] to cyclic tetramers in the broad liquid bands of the IL and the IL/ML mixtures. Our combined experimental and theoretical approach for the gas and the liquid phases thus provides a quantitative understanding of the competition between differently H-bonded and charged constituents in liquids.

### **Acknowledgements**

MAJ thanks the Department of Energy (DOE) under grant DE-FG02-06ER15800 for support of this work. The cryogenic ion spectrometer critical to these measurements was provided by the Air Force Office of Scientific Research (AFOSR) under grants FA9550-17-1-0267 (DURIP) and FA9550-18-1-0213. RL thanks for the financial support from the Deutsche Forschungsgemeinschaft (DFG) under grant LU 506/14-1. TN and AS thank the “HERMES-Forschungsförderung” and the “Frauenförderprogramm” of the University of Rostock for supporting their research stays at Yale University.

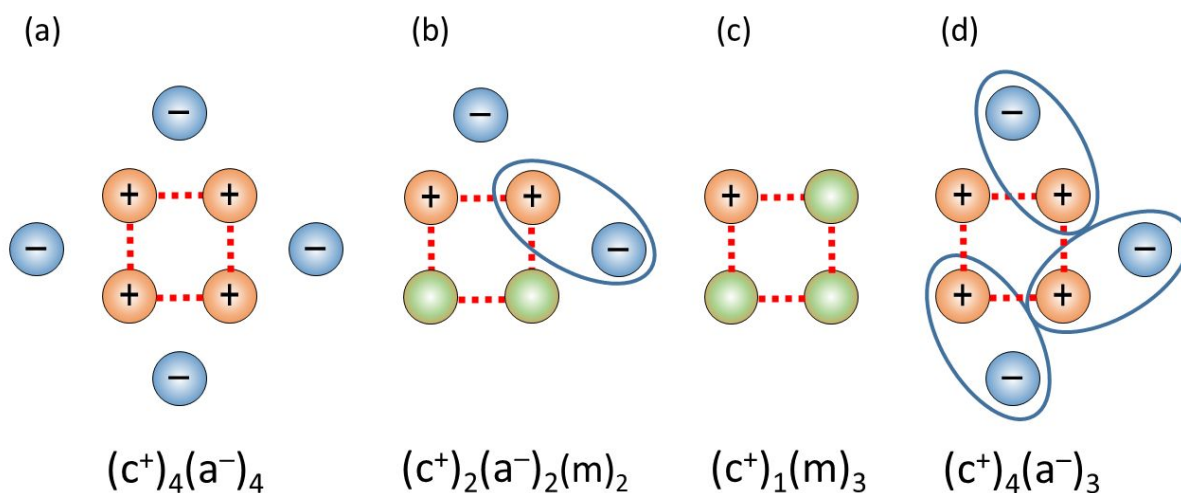
## References

1. M. L. Huggins, *Science* **1922**, 55, 459-460.
2. W. M. Latimer, W. H. Rodebush, *J. Am. Chem. Soc.* **1920**, 42, 1419-1433.
3. M. L. Huggins, *Angew. Chem., Int. Ed.* **1971**, 10, 147-152; *Angew. Chem.* **1971**, 83, 163-168.
4. L. Pauling, *The Nature of the Chemical Bond and the Structure of Molecules and Crystals: An Introduction to Modern Structural Chemistry*, Cornell University Press, Ithaca, N.Y., **1960**.
5. G. A. Jeffrey, *An Introduction to Hydrogen Bonding*, Oxford University Press, New York, **1997**.
6. G. Gilli, P. Gilli, *The Nature of the Hydrogen Bond: Outline of a Comprehensive Hydrogen Bond Theory*, Oxford University Press, Oxford, **2009**.
7. G. R. Desiraju, T. Steiner, *The Weak Hydrogen Bond: In Structural Chemistry and Biology*, Oxford University Press, Oxford, **1999**.
8. Y. Maréchal, *The Hydrogen Bond and the Water Molecule: The Physics and Chemistry of Water, Aqueous and Bio-Media*, Elsevier, Amsterdam ; Boston, **2007**.
9. T. Steiner, *Angew. Chem., Int. Ed.* **2002**, 41, 48-76; *Angew. Chem.* **2002**, 114, 50-80.
10. A. C. Legon, *Chem. Soc. Rev.* **1993**, 22, 153-163.
11. H. Weingärtner, *Angew. Chem., Int. Ed.* **2008**, 47, 654-670; *Angew. Chem.* **2008**, 120, 664-682.
12. F. Endres, S. Z. El Abedin, *Phys. Chem. Chem. Phys.* **2006**, 8, 2101-2116.
13. T. Welton, *Chem. Rev.* **1999**, 99, 2071-2083.
14. N. V. Plechkova, K. R. Seddon, *Chem. Soc. Rev.* **2008**, 37, 123-150.
15. S. P. M. Ventura, F. A. E. Silva, M. V. Quental, D. Mondal, M. G. Freire, J. A. P. Coutinho, *Chem. Rev.* **2017**, 117, 6984-7052.
16. M. Galiński, A. Lewandowski, I. Stępnia, *Electrochim. Acta* **2006**, 51, 5567-5580.
17. S. Menne, J. Pires, M. Anouti, A. Balducci, *Electrochem. Commun.* **2013**, 31, 39-41.
18. K. Fumino, R. Ludwig, *J. Mol. Liq.* **2014**, 192, 94-102.
19. K. Fumino, S. Reimann, R. Ludwig, *Phys. Chem. Chem. Phys.* **2014**, 16, 21903-21929.
20. K. Fumino, A. Wulf, R. Ludwig, *Angew. Chem., Int. Ed.* **2008**, 47, 8731-8734.
21. K. Fumino, T. Peppel, M. Geppert-Rybczyńska, D. H. Zaitsau, J. K. Lehmann, S. P. Verevkin, M. Köckerling, R. Ludwig, *Phys. Chem. Chem. Phys.* **2011**, 13, 14064-14075.

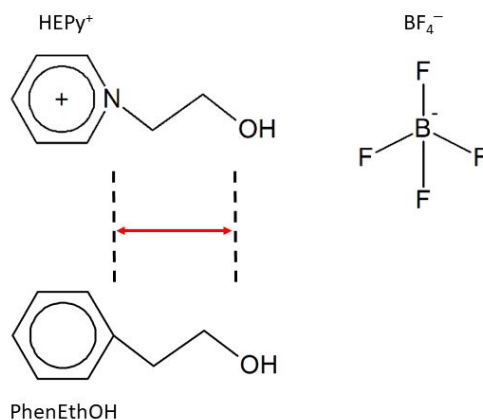
22. P. A. Hunt, C. R. Ashworth, R. P. Matthews, *Chem. Soc. Rev.* **2015**, 44, 1257-1288.
23. C. R. Ashworth, R. P. Matthews, T. Welton, P. A. Hunt, *Phys. Chem. Chem. Phys.* **2016**, 18, 18145-18160.
24. R. Ozawa, S. Hayashi, S. Saha, A. Kobayashi, H. Hamaguchi, *Chem. Lett.* **2003**, 32, 948-949.
25. H. Katayanagi, S. Hayashi, H. Hamaguchi, K. Nishikawa, *Chem. Phys. Lett.* **2004**, 392, 460-464.
26. J. D. Holbrey, W. M. Reichert, M. Nieuwenhuyzen, S. Johnston, K. R. Seddon, R. D. Rogers, *Chem. Commun.* **2003**, 1636-1637.
27. A. Triolo, O. Russina, V. Arrighi, F. Juranyi, S. Janssen, C. M. Gordon, *J. Chem. Phys.* **2003**, 119, 8549-8557.
28. R. W. Berg, M. Deetlefs, K. R. Seddon, I. Shim, J. M. Thompson, *J. Phys. Chem. B* **2005**, 109, 19018-19025.
29. Y. Umebayashi, T. Fujimori, T. Sukizaki, M. Asada, K. Fujii, R. Kanzaki, S. Ishiguro, *J. Phys. Chem. B* **2005**, 109, 8976-8982.
30. K. Fujii, T. Fujimori, T. Takamuku, R. Kanzaki, Y. Umebayashi, T. Sukizaki, R. S. Ishiguro, *J. Phys. Chem. B* **2006**, 110, 8179-8183.
31. T. Köddermann, C. Wertz, A. Heintz, R. Ludwig, *ChemPhysChem*, **2006**, 7, 1944-1949.
32. A. Yokozeke, D. J. Kasprzak, M. B. Shiflett, *Phys. Chem. Chem. Phys.* **2007**, 9, 5018-5026.
33. S. A. Katsyuba, M. V. Vener, E. E. Zvereva, Z. F. Fei, R. Scopelliti, G. Laurenczy, N. Yan, E. Paunescu, P. J. Dyson, *J. Phys. Chem. B* **2013**, 117, 9094-9105.
34. A. Knorr, R. Ludwig, *Sci. Rep.* **2015**, 5, 17505.
35. A. Knorr, P. Stange, K. Fumino, F. Weinhold, R. Ludwig, *ChemPhysChem* **2016**, 17, 458-462.
36. A. Strate, T. Niemann, D. Michalik, R. Ludwig, *Angew. Chem., Int. Ed.* **2017**, 56, 496-500.
37. T. Niemann, D. Zaitsau, A. Strate, A. Villinger, R. Ludwig, *Sci. Rep.* **2018**, 8, 14753.
38. F. S. Menges, H. J. Zeng, P. J. Kelleher, O. Gorlova, M. A. Johnson, T. Niemann, A. Strate, R. Ludwig, *J. Phys. Chem. Lett.* **2018**, 9, 2979-2984.
39. T. Niemann, A. Strate, R. Ludwig, H. J. Zeng, F. S. Menges, M. A. Johnson, *Angew. Chem., Int. Ed.* **2018**, 57, 15364-15368; *Angew. Chem.* **2018**, 130, 15590-15594.
40. M. Fakhraee, B. Zandkarimi, H. Salari, M. R. Gholami, *J. Phys. Chem. B* **2014**, 118,

14410-14428.

41. S. K. Panja, B. Haddad, J. Kiefer, *ChemPhysChem* **2018**, 19, 3061-3068.
42. F. N. Keutsch, R. J. Saykally, *Proc. Natl. Acad. Sci. U. S. A.* **2001**, 98, 10533-10540.
43. R. Ludwig, *Angew. Chem., Int. Ed.* **2001**, 40, 1808-1827.
44. F. Huisken, M. Stemmler, *Chem. Phys. Lett.* **1988**, 144, 391-395.
45. H. L. Han, C. Camacho, H. A. Witek, Y. P. Lee, *J. Chem. Phys.* **2011**, 134, 144309.
46. P. Ayotte, G. H. Weddle, M. A. Johnson, *J. Chem. Phys.* **1999**, 110, 7129-7132.
47. Gaussian 09, Revision D.01, M. J. Frisch, G. W. Trucks, H. B. Schlegel, G. E. Scuseria, M. A. Robb, J. R. Cheeseman, G. Scalmani, V. Barone, B. Mennucci, G. A. Petersson, et al.
48. C. Møller, M. S. Plesset, *Phys. Rev.* **1934**, 46, 618-622.
49. M. Head-Gordon, J. A. Pople, M. J. Frisch, *Chem. Phys. Lett.* **1988**, 153, 503-506.
50. A. Strate, T. Niemann, R. Ludwig, *Phys. Chem. Chem. Phys.* **2017**, 19, 18854-18862.
51. A. Strate, V. Overbeck, V. Lehde, J. Neumann, A. M. Bónsa, T. Niemann, D. Paschek, D. Michalik, R. Ludwig, *Phys. Chem. Chem. Phys.* **2018**, 20, 5617-5625.
52. M. Okumura, L. I. Yeh, J. D. Myers, Y. T. Lee, *J. Phys. Chem.* **1990**, 94, 3416-3427.
53. A. B. Wolk, C. M. Leavitt, E. Garand, M. A. Johnson, *Acc. Chem. Res.* **2014**, 47, 202-210.
54. C. J. Johnson, J. A. Fournier, C. T. Wolke, M. A. Johnson, *J. Chem. Phys.* **2013**, 139, 224305.
55. J. A. Fournier, C. T. Wolke, C. J. Johnson, A. B. McCoy, M. A. Johnson, *J. Chem. Phys.* **2015**, 142, 064306.
56. S. M. Craig, F. S. Menges, M. A. Johnson, *J. Mol. Spectrosc.* **2017**, 332, 117-123.
57. F. S. Menges, S. M. Craig, N. Totsch, A. Bloomfield, S. Ghosh, H. J. Kruger, M. A. Johnson, *Angew. Chem., Int. Ed.* **2016**, 55, 1282-1285.
58. K. Liu, M. G. Brown, J. D. Cruzan, R. J. Saykally, *Science* **1996**, 271, 62-65.
59. K. Nauta, R. E. Miller, *Science* **2000**, 287, 293-295.



**Scheme 1.** Illustrations explaining the concept of this study. The identification of the structural motifs can be achieved by liquid and gas phase IR spectroscopies. (a) Cyclic tetramers  $(c^+)_4(a^-)_4$ , fully compensated by counter anions in the neutral bulk system. (b) Neutral cyclic tetramers  $(c^+)_2(a^-)_2(m)_2$  in the bulk phase, wherein ion-pairs  $(c^+)(a^-)$  (circled in (b)) are replaced by molecules (m). (c) Positively charged cyclic tetramers  $(c^+)(m)_3$  in the gas phase. (d) Positively charged cyclic tetramers  $(c^+)_4(a^-)_3$  in the gas phase, with stronger Coulomb repulsion by removing one counter anion.



**Scheme 2.** The 1-(2-hydroxyethyl)pyridinium (HEPy<sup>+</sup>) cation and the tetrafluoroborate (BF<sub>4</sub><sup>-</sup>) anion as constituents of [HEPy][BF<sub>4</sub>] IL. The molecular mimic of the cation, 2-phenylethanol (PhenEthOH), has a similar distance between the aromatic ring and the hydroxyl group as indicated by the red double-headed arrow.

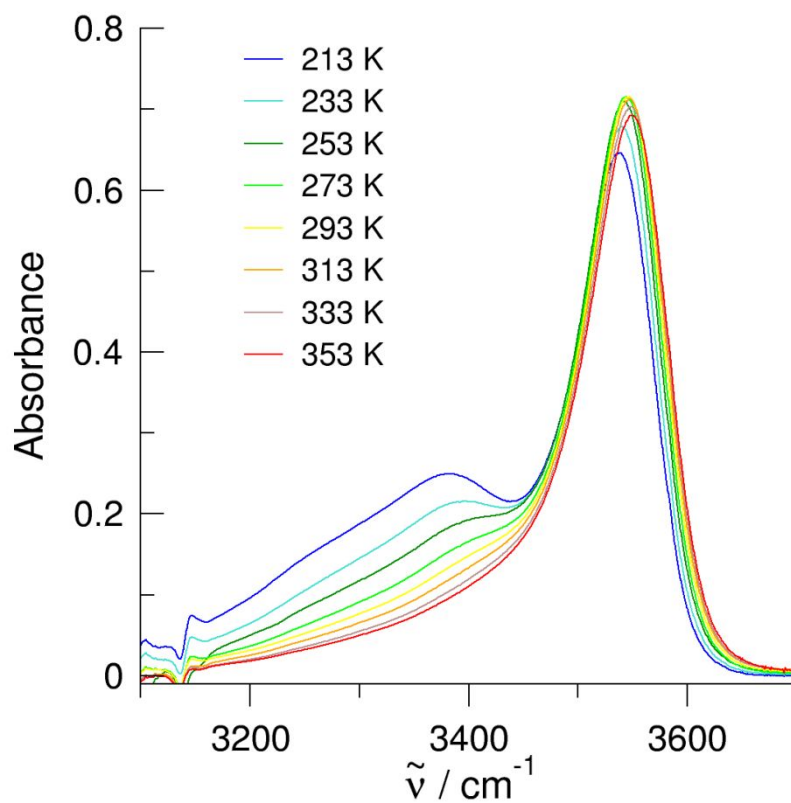


**Figure 1.** Infrared difference spectra in the OH stretch region of [HEPy][BF<sub>4</sub>] as a function of temperature between 213 K and 353 K. The spectra of the OD functionalized IL are subtracted from the corresponding spectra of the all-H species to remove the CH stretches of the pyridinium ring and exclude interference between CH and OH contributions.

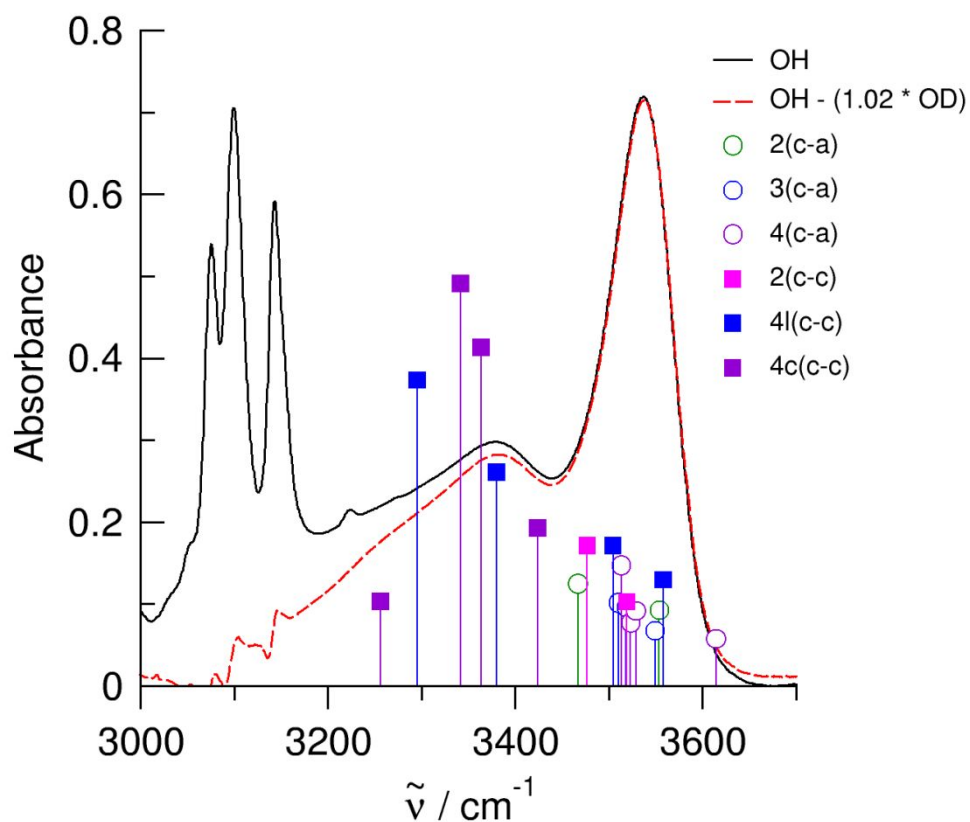


**Figure 2.** Calculated frequencies [B3LYP-D3/6-31+G\*, scaled by 0.985] of (c-a) (open symbols) and (c-c) (filled symbols) clusters, compared to the IR spectrum of [HEPy][BF<sub>4</sub>] (solid black line) as well as the IR difference spectrum of IL-OH/IL-OD (red dashed line) at 213 K. Both linear and cyclic (c-c) configurations were considered. The (c-c) feature of the bulk liquid spectra is best represented by the cyclic tetramers (4c(c-c)).

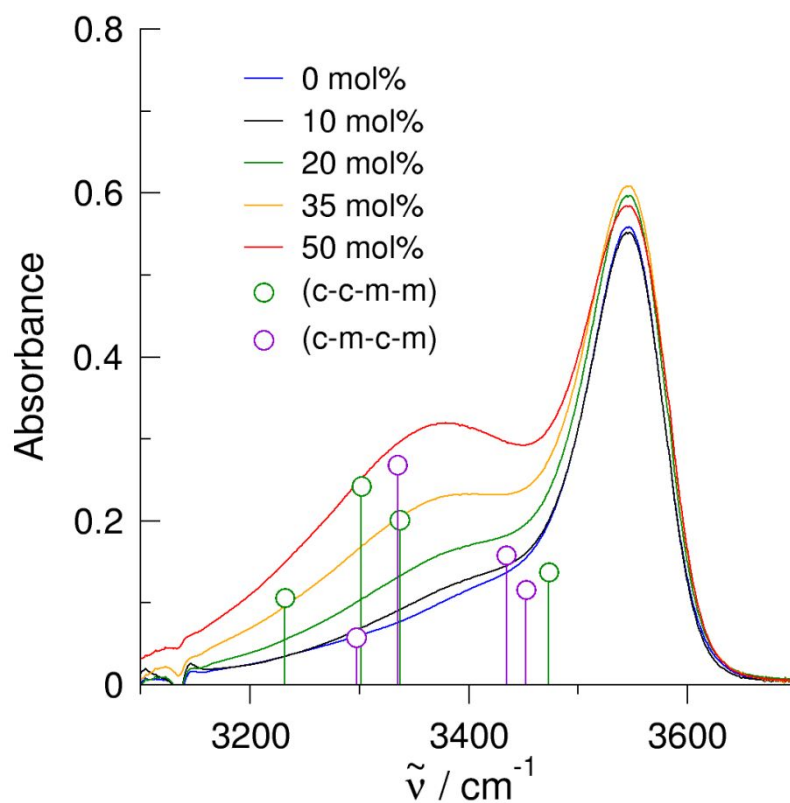


**Figure 3.** Infrared spectra in the OH stretch region of [HEPy][BF<sub>4</sub>]/PhenEthOH mixtures measured at different concentrations of 2-phenylethanol at 293 K. Calculated neutral tetramer cluster structures are provided in Fig. S1.

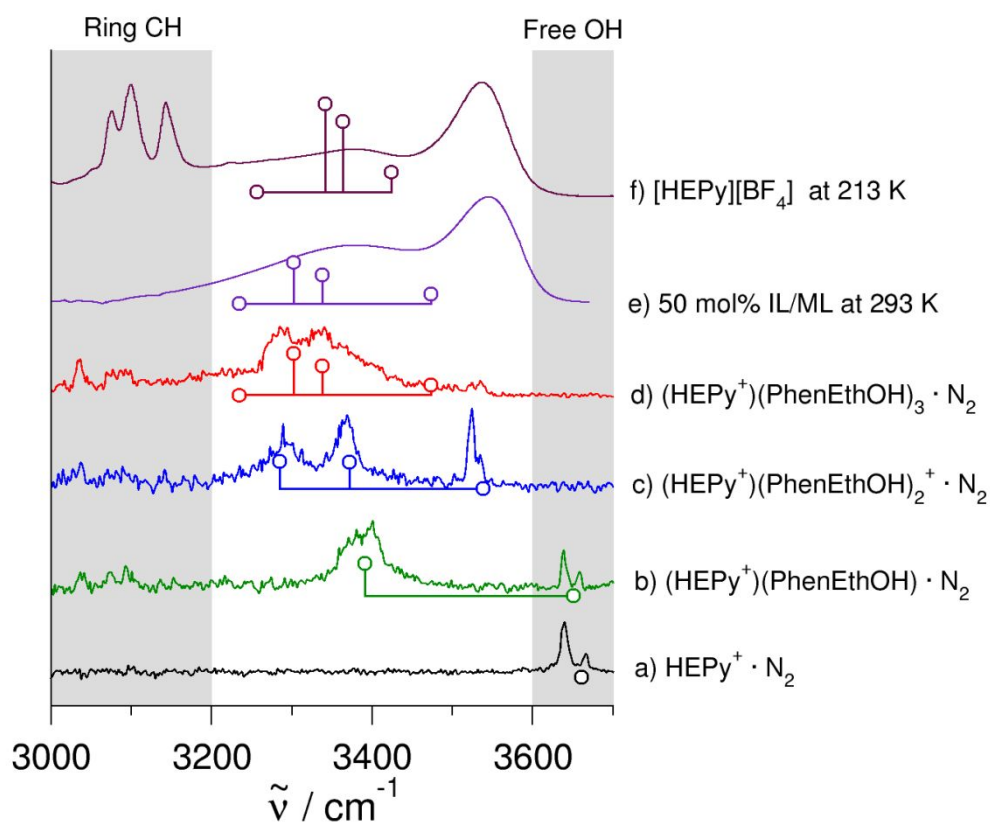


**Figure 4.** Vibrational predissociation spectra of  $N_2$ -tagged cation  $HEPy^+$  (black) along with those of the  $(HEPy^+)(PhenEthOH)_n$  clusters with  $n = 1$  (green),  $n = 2$  (blue) and  $n = 3$  (red) at  $\sim 35$  K. The bulk liquid IR spectra of the 50 mol% mixture of  $[HEPy][BF_4]/PhenEthOH$  at 293 K (purple) and the pure ionic liquid  $[HEPy][BF_4]$  at 213 K (teal). For comparison, the calculated frequencies of the monomer, dimer and the corresponding cyclic trimer and tetramers (see Scheme 1(a), (c) and (d)) are provided whereby the lowest intensities are set to zero.

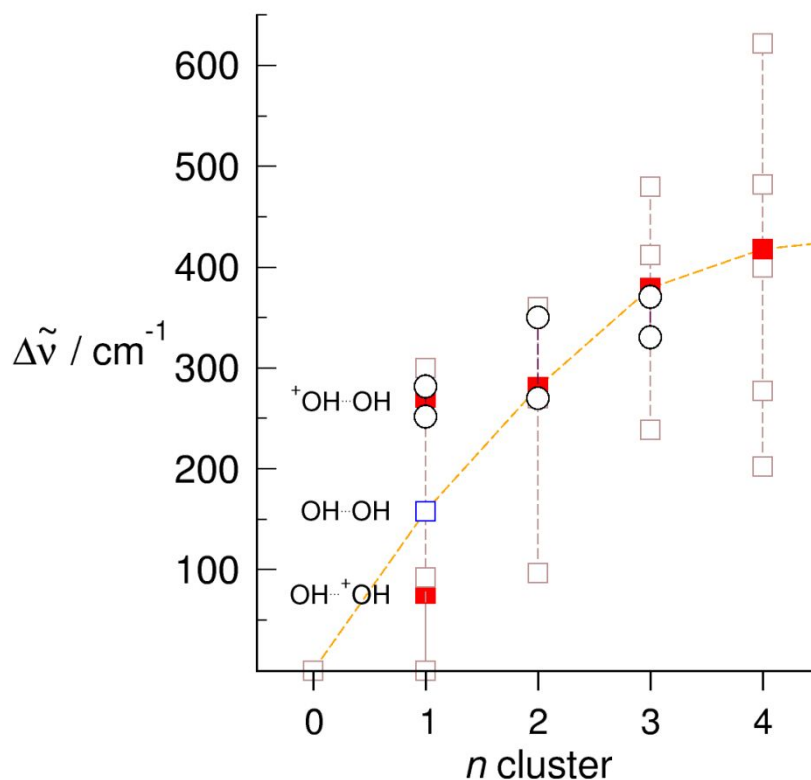


**Figure 5.** Calculated vibrational redshifts for two kinds of binary complexes  $(\text{HEPy}^+)(\text{PhenEthOH})$  compared to the alcohol dimer  $(\text{PhenEthOH})_2$ , and the cyclic clusters  $(\text{HEPy}^+)(\text{PhenEthOH})_n$  with  $n = 2-4$ . We calculated the shifts relative to the OH stretches of the bare cation  $\text{HEPy}^+$  (brown squares). The intensity weighted average frequencies (filled red squares) are guided by the dashed orange line. The single blue square symbolizes the OH red shift of the alcohol dimer  $(\text{PhenEthOH})_2$ . The experimentally observed bands in the gas phase spectra appear at the frequencies calculated for the cyclic trimer  $(\text{HEPy}^+)(\text{PhenEthOH})_2$  and cyclic tetramer  $(\text{HEPy}^+)(\text{PhenEthOH})_3$  (black open circles).

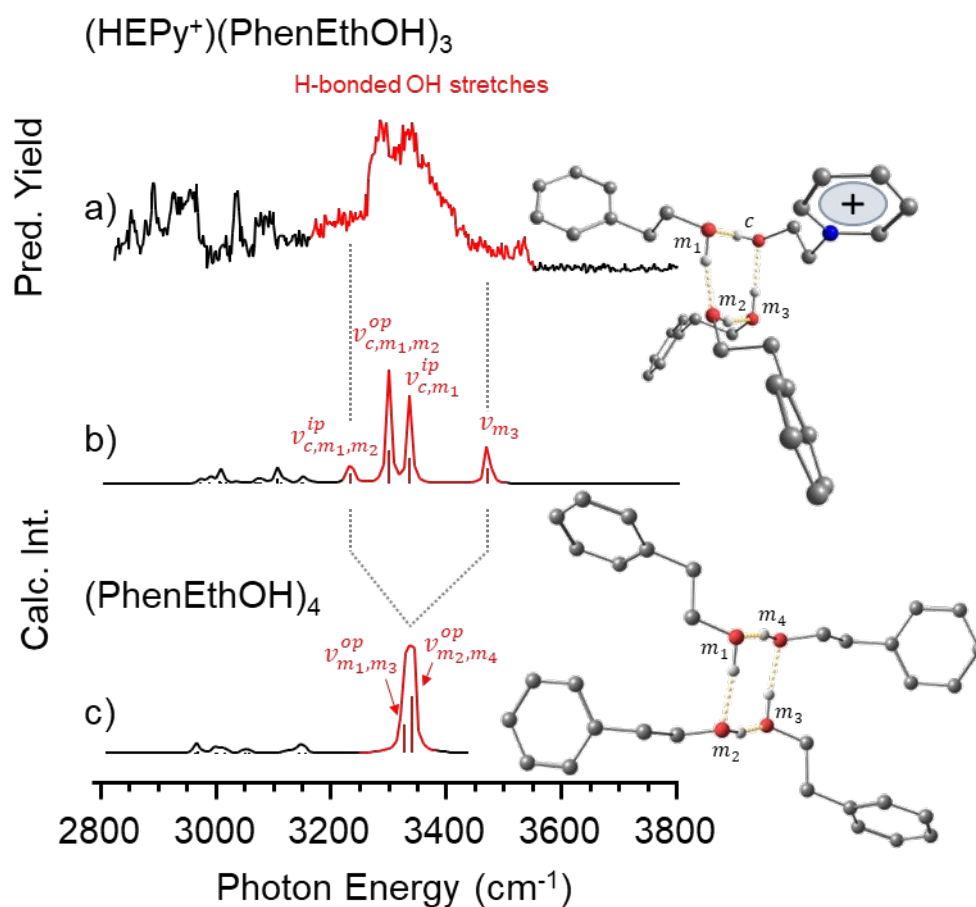


**Figure 6.** Vibrational predissociation spectra of N<sub>2</sub>-tagged (a) (HEPy<sup>+</sup>)(PhenEthOH)<sub>3</sub>, compared to (b) its calculated spectrum. Calculated spectrum of (c) the cyclic molecular mimic tetramer (PhenEthOH)<sub>4</sub> is also presented for comparison. The superscripts ‘ip’ and ‘op’ in the band labels stands for ‘in-plane’ and ‘out-of-plane’ stretches, respectively. The structures are provided on the right of the figure and H-atoms connected to carbon atoms are omitted for clarity.